Patient-specific Cardiovascular Modeling System Using the Immersed Boundary Technique

Wee-Beng Tay[a], Yu-Heng Tseng [a,*], Liang-Yu Lin[b] and Wen-Yih Tseng[c]

[a]*High Performance Computing & Environmental Fluid Dynamic Laboratory, Department of Atmospheric Sciences, National Taiwan University, Taipei, Taiwan (yhtseng@as.ntu.edu.tw)*
[b]*National Taiwan University Hospital, Taipei, Taiwan*
[c]*Center for Optoelectronic Biomedicine, National Taiwan University College of Medicine, Taipei, Taiwan*

Abstract. A three-dimensional (3-D), computational fluid dynamics (CFD) based, patient-specific cardiovascular modeling system is under-developed. The system aims to identify possible diseased conditions and facilitate physicians' diagnosis at early stage through the hybrid CFD simulation and time-resolved magnetic resonance imaging (4-D MRI). The CFD simulation is based on the 3-D heart model code originally developed by McQueen and Peskin, which can simultaneously compute fluid and elastic boundary motions using the immersed boundary method. This allows us to flexibly investigate the flow features in the ventricles and their responses. The simulation accuracy has been verified with clinical data. Results indicate that the variation of flow rates and kinetic energy have been well captured during the diastole and systole phase. The encouraging results indicate the feasibility of capturing important characteristics of the heart during different phases. However, some discrepancies are found in the pulmonary vein and aorta flow rate between the numerical and experimental data. Further studies are essential to investigate and solve the remaining problems before it can be used in the clinical diagnostics.

Keywords: Blood flow, Cardiovascular disease, Magnetic resonance imaging, Left ventricle, Numerical simulation, Vortices
PACS: 47.63.-b, 47.32.C-, 47.11.Bc, 87.19.U-

1. Introduction

A three dimensional (3-D), computational fluid dynamics (CFD) based, patient-specific cardiovascular modeling system is under-developed. A successful cardiovascular modeling system (CMS) should identify possible diseased conditions and facilitate physicians' diagnosis at early stage, which can be achieved through the hybrid CFD simulation and time-resolved magnetic resonance imaging (MRI) before heart failure.

Early research [1] has pointed out that the flow dynamics found in the left ventricle (LV) can reveal important information about the overall cardiac health. This is useful in the early diagnostic of patients with potential heart problems. In fact, the emphasis on the LV of the heart dates back to the 1970s. Early experimental studies found that there is eddy generation in the LV during ventricular filling. It was then thought to cause the early partial closure that prevents regurgitation [2]. However, later studies [3, 4] show that the valve closure is due to the developing adverse pressure gradient and the flow decelerates well before the flow reverses. Computational studies to investigate natural or prosthetic mitral valve are conducted by Mcqueen and Peskin [5] as early as 1982. Mcqueen and Peskin [6] later successfully developed a 3-D heart simulation based on idealized hemodynamic conditions. In order to accommodate the complex geometries, moving wall and fluid-tissue interaction, the immersed boundary method (IBM) is used. Detailed investigation can be conducted through the simulation of blood flow in the heart over a cardiac cycle. This approach is much more suitable than other numerical methods based on structured or unstructured grids since it allows for large grid deformation and is efficient. With appropriate data on the flow rates and pressures of the heart at different times throughout a cycle, one will be able to visualize and detect any peculiarities which occur within the heart in the simulation. The flow pattern within the ventricles of the heart can also be analyzed in detail.

Vortex formation in LV has also attracted much attention recently. Fortini et al. [7] experimentally investigated the effect of mechanical heart valves (MHV) on the flow characteristic of the blood inside a modeled LV. The three types of tested MHV are (a) a one-way, hydraulic valve; (b) a monoleaflet valve; and (c) a bileaflet valve. The first configuration most resembles the natural valve while the modeled LV is a silicone rubber conical sack, which is flexible and transparent. A comparison of vorticity shows that valve (a) gives the simplest plot with just two oppositely signed vortices while the vorticity fields generated by valves (b) and (c) are more complicated. Four to five vortices are generated and are less orderly compared to the valve (a) case.

Other numerical studies of flow within LV also showed the complexity of vortex formation. Domenichini et al. [8] used a mixed spectral-finite differences method to simulate the 3-D fluid dynamics inside the LV of the heart during diastole. They analyzed the sensitivities of several governing parameters, including the eccentricity, Stokes number and Strouhal number. It was found that there is a well-defined structure of vortices regardless of these parameters. As the eccentricity increases, the flow field changes smoothly from almost axisymmetric to complex 3-D structures when the values are similar to the physiological ones. The effect of Stokes number on the flow is rather weak. On the other hand, as Strouhal number decreases, the effect of convection increases and the entry jet extends more deeply into the ventricle. Instability may follow and result in weak turbulence. However, their simplified model only comprises of the LV of the heart. Hence, a more sophisticated simulation including the entire 3-D heart and detailed inflow/outflow information is required. Nevertheless, their analysis theoretically presented the possible flow structure associated with different parameters.

Saber et al. [9] further made use of patient-specific MRI images to construct the geometry of the LV of a 3-D heart in the numerical simulation. Hence, the geometry of the LV at different instances is prescribed rather than influenced by the FSI. The valves of LV are represented by 2-D planar models. The simulation is based on another commercial CFD solver, Star-CD. In Saber et al. [13], the inflow/outflow rate at the mitral/aortic valves cannot be specified as boundary condition due to the limited measurements. Therefore, a uniform, constant pressure is prescribed at the mitral and aortic valves. Their model is able to capture the 3-D contraction and expansion phases of the LV. However, areas of the mitral and aortic valves are underestimated with overestimated velocities. This could be due to the low resolution of MRI and interpolation uncertainties. Saber et al. [9] indicated the importance of clear MRI images to construct the geometry of LV in the simulation. However, it is common to retrieve MRI images with blurring or ghosting artifacts in reality due to breathing motion and bowel movement [10]. Particularly for time-resolved 3-D data acquisitions, large amounts of data require measurement durations that often exceed normal human breath-holding capabilities. These poor quality images will hinder an accurate analysis of the heart. Markl et al. [11] used an improved navigator-gated time-resolved 3-D phase contact MRI (PC-MRI) velocity mapping based on real-time adaptive k-space reordering in combination with a wider data acceptance window to improve the image quality. The acquisition of images is achieved using an eight-channel phased-array body coil (3T system, TRIO; Siemens, Erlangen, Germany [11]) . This system allows one to reconstruct the 3-D images of the heart over a cardiac cycle as well as time-resolved 3-D hemodynamic velocity fields. In general, the appearances of images are excellent with moderate blurring and minor ghosting artifacts. Currently, available data comprises of both healthy volunteer as well as patients with cardiac problems for comparison in the hospital.

The main objective of this study is to develop a 3-D CFD based, patient-specific cardiovascular modeling system. The tools comprise of a 3-D CFD model to simulate the heart and the 4-D PC-MRI system. This hybrid system could potentially identify possible diseased conditions in LV through the analysis of the vorticity, kinetic energy, hemodynamic, pressure and shear stress. This facilitates physicians to diagnose any probable cardiac problems at an early stage. For example, it has been estimated that about 30% of all heart attacks are fatal [12]. In this way, sudden heart attacks can be avoided and more lives can be saved. Similar to Saber et al. [9], both MRI images and CFD simulation are used in this study. This paper mainly focuses on the accurate model representation of the heart flow within the cardiac cycle and the resulting vortex dynamics in the LV. In order to achieve better accuracy, we take the advantage of the IBM code described by Mcqueen and Peskin [6] rather than a commercial software. The IBM is more suitable for this large movement simulation since it does not suffer from grid quality deterioration, commonly seen in structured grids. Furthermore, the entire heart is simulated in our study. This heart model is constructed based on the anatomy and mechanical properties of the heart muscle fibers, which have been extensively documented by physiologists. It can, therefore, be easily incorporated into any computer model. More details can be found in McQueen and Peskin [6]. Moreover, the moving geometry of the heart (or LV) is changed with time according to the FSI between fluids and muscles. Hence it is more accurate to simulate the changing geometry of the heart.

As a first step, we concentrate on the verification of the IBM model with clinical data. The next section describes the methodology of the cardiovascular modeling system, followed by a detailed description of the 4-D PC-MRI system and its capabilities. The numerical method developed by Mcqueen and Peskin [6] will be explained briefly. Our results involved hemodynamic comparison, vortex and kinetic energy analysis. Good agreement has been

obtained in most cases. The conclusion summarizes the overall performance and specific areas which require further investigation.

2. Methods

2.1 Patient-specific Cardiovascular Modeling System

In order to develop an accurate CFD based, patient-specific cardiovascular modeling system, we need to integrate the analyzed data from 4-D PC-MRI system (hardware) into the IBM heart model (software). The system details will be given in later sections. Fig. 1a) shows the fundamental methodology. Healthy volunteers, as well as patients with cardiac problems, have been requested to be scanned by the 4-D PC-MRI system. The raw data comprises of the images and the hemodynamic velocity of the heart over an entire cardiac cycle. The 3-D IBM heart model [6] requires the initial and boundary conditions for the pressure. This can be obtained from idealized cases as well as typical estimation of healthy adults documented in the medical literature. This allows us to investigate various scenarios and their effects on the LV of the heart. The quasi-realistic simulation provides very useful heart flow information for diagnostic, such as visualization, velocity field, kinetic energy (KE), vorticity and pressure. The comparison between volunteers and patients can help us to identify critical flow conditions resulting from diseased heart and provide deeper insights in the diagnostics.

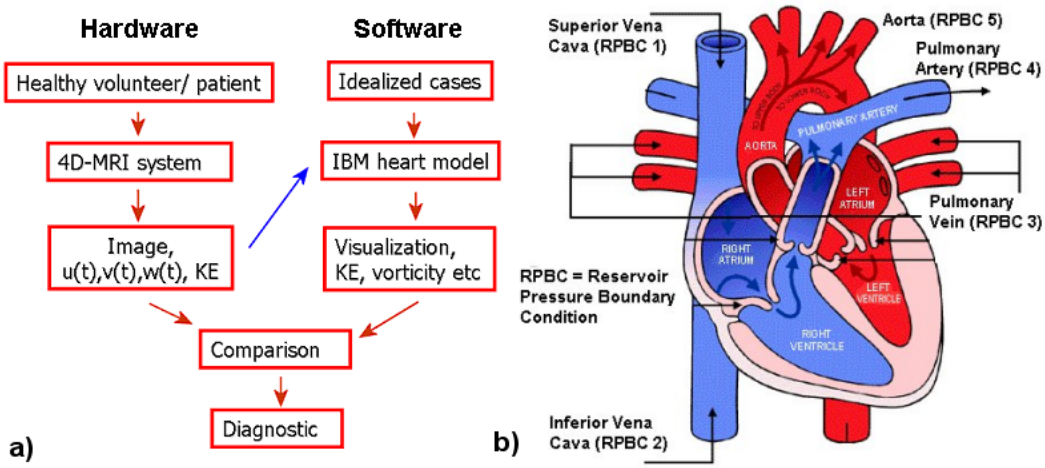

Fig. 1. a) Fundamental methodology of the CFD based, patient-specific cardiovascular modeling system b) Diagram of the heart with the five BC sources. (Figure modified from Abdallah [13])

In the CMS, the boundary conditions are specified at five major inflow and outflow sources, comprising of 1) superior vena cava (SVC); 2) inferior vena cava (IVC); 3) pulmonary vein (PV); 4) pulmonary artery (PA); and 5) aorta, as shown in Fig. 1b. These five sources primarily dictate how the blood flows in/out of the heart. It is crucial to specify them accurately. The SVC and IVC are two large veins in charge of transporting de-oxygenated blood to the right atrium of the heart respectively [14]. The SVC is formed by the left and right brachiocephalic veins and blood through the SVC enters the right atrium through the upper right front of the heart. Similarly, the blood in the IVC enters through the lower right, back side of the heart. The PV (four in reality, but simplified to only one in the 3-D heart model) carries oxygenated blood from the lungs to the left atrium (LA) of the heart. It delivers de-oxygenated blood from the heart to the lungs. The aorta, the largest blood vessel in the body which originates from the LV of the heart, transports oxygenated blood to all parts of the body. Early research [8, 15, 16] has shown that the filling dynamics of LV contains vital health information of the heart. We, therefore, concentrate on the flow dynamics of the LV and the PV in this study, which directly affects the blood entering the LV.

2.2 4-D PC-MRI System

The latest 4-D time-resolved PC-MRI, located at the National Taiwan University Hospital, provides better and more realistic physiological information for the CFD flow simulation. This system acquires images using an eight-channel phased-array body coil, which allows the reconstruction of 3-D images of the heart over a cardiac cycle. However, getting clear and accurate images is not straightforward due to various problems, such as insufficient respiration control, artifact generation and limited signal-to-noise ratio [11]. Moreover, post-processing will be required to identify, check and extract the relevant heart flow fields over the cardiac cycle. The images are taken at intervals of approximately 45 milliseconds. The spatial resolution of the each image is 256x192x8 (x,y,z), which approximates to an actual size of 307x230x48 mm. Each "z=" plot represents the z coordinate slice of the xy plane.

The test subjects of the 4-D PC-MRI system comprise of both healthy volunteer as well as patients with cardiac problems. This will enable a distinct comparison between the two groups of participants. However, in our initial test and hereafter, we took the data from a healthy volunteer, 35 year-old female. A snapshot image is shown in Fig. 2 taken at T=0.2, where 1T is equivalent to a whole heartbeat. This is one of the heart image slices at the resolution of 256x192. The colored arrows indicate the velocity vectors of the blood flow. A high concentration of vectors is observed in the circled region and this corresponds to the diastolic phase when large amounts of blood enter the LV.

As mentioned earlier, some researches have emphasized on the distinct differences between the vortex formation process in the LV of the heart for the healthy volunteer as well as patients with cardiac problems. With the aid of our CFD heart model, we can now investigate closely the entire process happening within the LV. The final objective is to examine whether disease-related dysfunctions in intervals before complete heart failure can be observed in the dynamics of transmitral blood flow during early LV diastole. Combing the non-invasive 4-D PC-MRI information with the quasi-realistic heart model provides us a unique opportunity to evaluate the cardiovascular hemodynamic in advance.

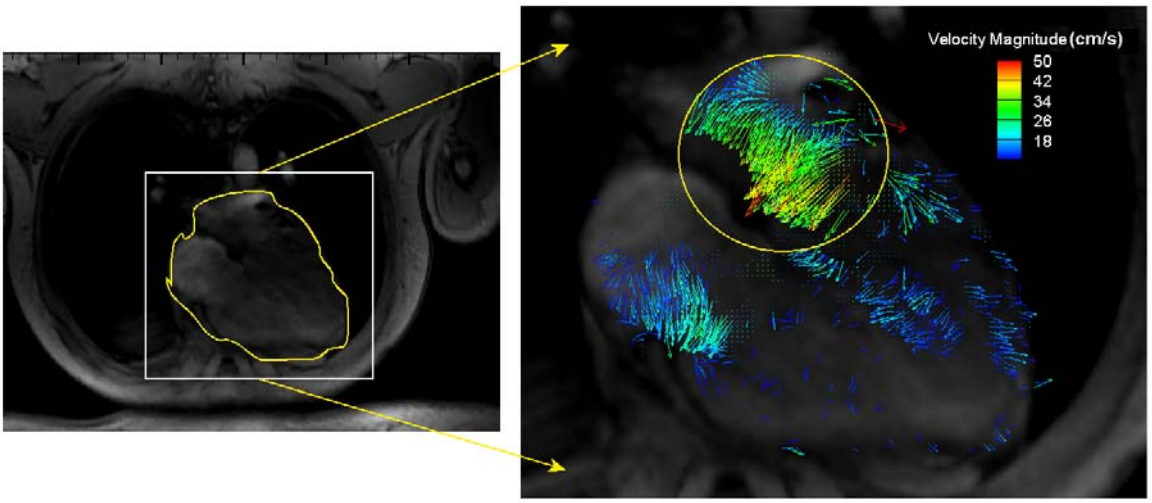

Fig. 2. One of the heart image slices at 256x192 resolution obtained using the 4-D PC-MRI system. The vector's color indicate its velocity magnitude.

2.3 3-D Cardiovascular Model and Numerical Method

The 3-D IBM heart simulation is based on the model developed by Mcqueen and Peskin [6]. This CMS is more adequate for modeling elastic and contractile fibers of the heart than other variations of the IBM [17, 18]. The governing equations are based on the 3-D incompressible Navier-Stokes equations with the immersed boundary forcing given by:

$$\rho\left(\frac{\partial \boldsymbol{u}}{\partial t} + \boldsymbol{u}\cdot\nabla\boldsymbol{u}\right) + \nabla p = \mu\Delta\boldsymbol{u} + \boldsymbol{f}\,, \tag{1}$$

$$\nabla\cdot\boldsymbol{u} = \boldsymbol{0}\,, \tag{2}$$

$$\boldsymbol{f}(\boldsymbol{x},t) = \int_0^{L_b} \boldsymbol{F}(s,t)\delta(\boldsymbol{x} - \boldsymbol{X}(s,t))ds\,, \tag{3}$$

$$\frac{\partial \boldsymbol{X}(s,t)}{\partial t} = \boldsymbol{u}(\boldsymbol{X}(s,t),t) = \int_\Omega \boldsymbol{u}(\boldsymbol{x},t)\delta(\boldsymbol{x} - \boldsymbol{X}(s,t))dx\,, \tag{4}$$

$$\boldsymbol{F}(s,t) = \boldsymbol{S}(\boldsymbol{X}(\cdot,t),t)\,. \tag{5}$$

In this case, $\boldsymbol{x} = (x,y,z)$, $\boldsymbol{u}(\boldsymbol{x},t) = (u_1(\boldsymbol{x},t), u_2(\boldsymbol{x},t), u_3(\boldsymbol{x},t))$, is the fluid velocity and $p(\boldsymbol{x},t)$ is the fluid pressure. μ and ρ represent the fluid viscosity and density respectively. The force density (with respect to $d\boldsymbol{x} = dxdydz$) acting on the fluid is $\boldsymbol{f}(\boldsymbol{x},t) = (f_1(\boldsymbol{x},t), f_2(\boldsymbol{x},t), f_3(\boldsymbol{x},t))$. $\boldsymbol{s}$ tracks a material point of the immersed boundary and the boundary force density (with respect to ds) is $\boldsymbol{F}(s,t) = (F_1(s,t), F_2(s,t), F_3(s,t))$.

Eq. (3) and (4) estimate the interaction between the immersed boundary and the fluid. Eq. (5) represents the boundary force resulting from the boundary configuration at time t, where the function $\boldsymbol{S}$ satisfies a generalized Hooke's law if the boundary is elastic.

Two sets of grids, fixed and moving, are adopted in the CMS. The fixed grid represents the Cartesian grid x,y,z which covers the entire fluid domain. On the other hand, the moving grid represents the boundary or fibers of the heart. At each time step, the force acting at each point on the fiber is calculated using Eq. (5). These fibers exert force onto the fluid, represented by the Cartesian fixed grid, and the force on the fluid is calculated using Eq. (3). The resulting velocity at time step ($n+1/2$) is then obtained by solving Eq. (1) and (2) using the fractional step method, which solves the momentum and the pressure Poisson equations. With this, one can return to interpolate the fiber's velocity from its surrounding fluid's velocity. The fibers then move to their new positions at $t=n+1/2$ based on their velocities. With the known velocities and positions of the fibers at $t=n+1/2$, the solution process is repeated but now they are used to take a full time step from $t=n$ to $n+1$. This results in a time-centered or Crank-Nicolson scheme which has "formal" second-order accuracy [19]. The whole process is shown in Fig. 3.

The construction of the 3-D IBM heart model includes a few steps. The most fundamental component is the boundary points, which are joined together to form fibers. Fibers with the same number of points are clustered together as a group while a bunch is made up of groups. The bunches together form the heart. Hence, the entire heart model is made up of about 4,000 fibers consisting of about 600,000 boundary points. On the other hand, the fixed Cartesian grid uses 128x128x128 grid points. A new single heartbeat, together with the initial transient, requires about 57,000 time steps. Subsequent heartbeats require about 32,000 time steps. The current simulation uses the first heartbeat after the initial transient since there are problems after around 57,800 time steps. This will be discussed in more details in the following paragraphs.

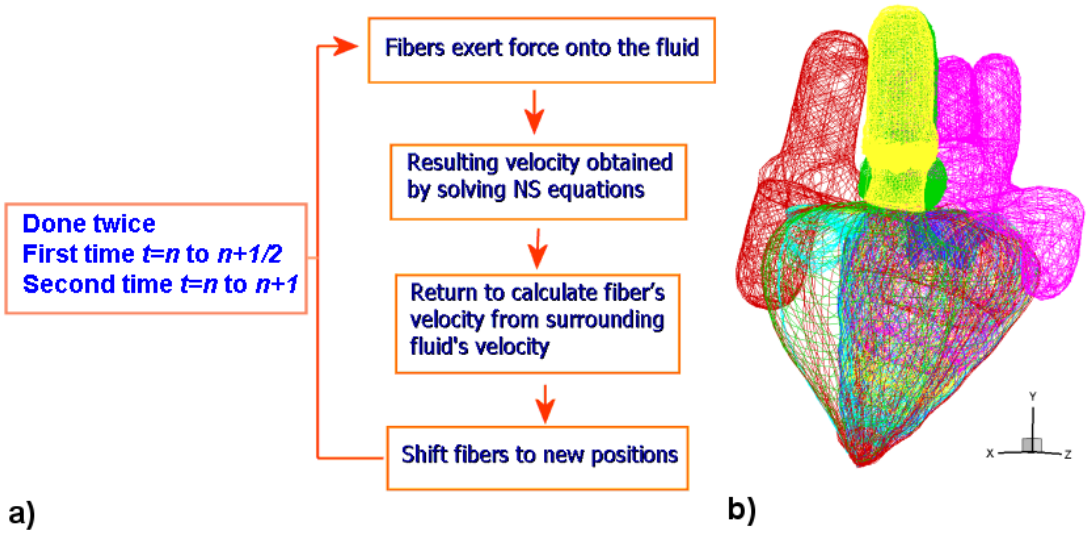

Fig. 3. a) Flowchart of the IBM numerical method and the b) 3-D IBM heart model

Similar to Mcqueen and Peskin [6], we impose a fixed reservoir pressure boundary condition (RPBC) throughout the cardiac cycle. This is similar to the boundary condition used by Saber et al. [9]. Table 1 shows the RPBC at the different sources of the heart.

A few full cardiac cycles are simulated in the current CMS. The LV is initially empty and requires to be filled up with sufficient blood. Otherwise, the simulation may not run successfully. This filling period runs from t=0 to 0.34s. Therefore, our analysis of the cardiac cycle starts from t=0.34 to t=1.14s (the whole cardiac cycle T lasts approximately 0.8 s). Hereafter, the time is normalized by the whole cardiac cycle (T=1.0) for simplicity. The simulation results are compared against clinical data in terms of hemodynamic, vorticity, and kinetic energy (KE).

Table 1. RPBC at different sources of the heart

Sources	SVC, IVC	PV	PA	Aorta
Reservoir pressure / mmHg	100	15	5	80

3. Results

3.1 Hemodynamic comparison

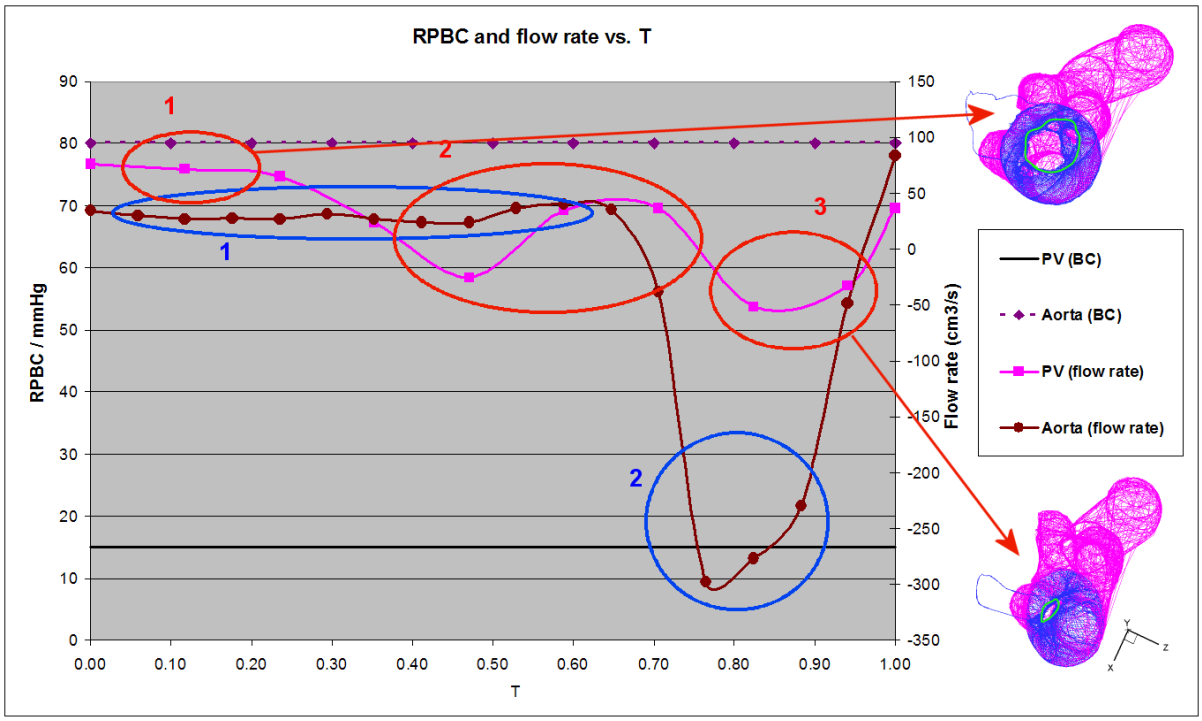

Fig. 4. PV and aorta RPBC/flow rate for one cardiac cycle

Fig. 4 shows the PV and aorta RPBC as well as their flow rate variation for one cardiac cycle. In the simulation, between T=0.0 and 0.25 (initial LV filling phase or also known as the E-wave [20], marked as red circle 1 in Fig. 4, the inflow rate at the PV is almost constant. Blood is entering the heart through the PV. At this time, the mitral valve in the simulation is also opened, as shown by the green circle at the top right hand side of Fig. 4. During the middle of the LV filling phase (just after T=0.4, red circle 2), the flow rate decreases, reverses and then increases again (circle 2, Fig. 4). This shows that some amount of blood is flowing out of the PV, resulting from a higher LA pressure due to the filled-up blood in LA. This is not surprising since the reservoir pressure is always constant. With the higher LA pressure now, backflow occurs and some blood begins to flow out, resulting in the negative PV flow

rate. After T=0.5, the inflow resumes again briefly. This corresponds to the second filling phase, or more commonly known as the A-wave [20], which is due to the atrial contraction. The earlier backflow has lowered the pressure in the LA and hence blood is flowing in again. However, the PV flow rate begins to decrease again after T=0.7. The diastole phase is ending and the systole phase is going to start. During systole, the inflow decreases to zero and changes to an outflow. A stronger outflow is again observed between T=0.75 to 1.0 (red circle 3, Fig. 4). This is again due to the higher pressure in the LA as a result of the earlier inflow of blood.

From Fig. 4, we can observe that at a constant aorta RPBC 80 mmHg, no significant difference is found in the flow rate of the aorta from T=0 to 0.65. This is because this period (blue circle 1) corresponds to the initial filling of blood in the LV. The pressure in the LV is still low compared to the aorta's pressure and hence only a small amount of inflow exists. After T=0.65, the systole phase begins (blue circle 2). During this period, large amount of oxygenated blood starts to flow out through the aorta to other parts of the body. In Fig. 5, the magnitude of the flow rate has been non-dimensionalized using the stroke volume* and the period of the cardiac cycle T and compared against the clinical data from Fortini et al. [7]. Baccani et al. [20] and Domenichini et al.[21] also have similar clinical data, except that their data is non-dimensionalized differently. Q represents the flow rate through the mitral during the diastole (0.00T–0.75T), and through the aortic valve during the systole (0.75T–1.00T).

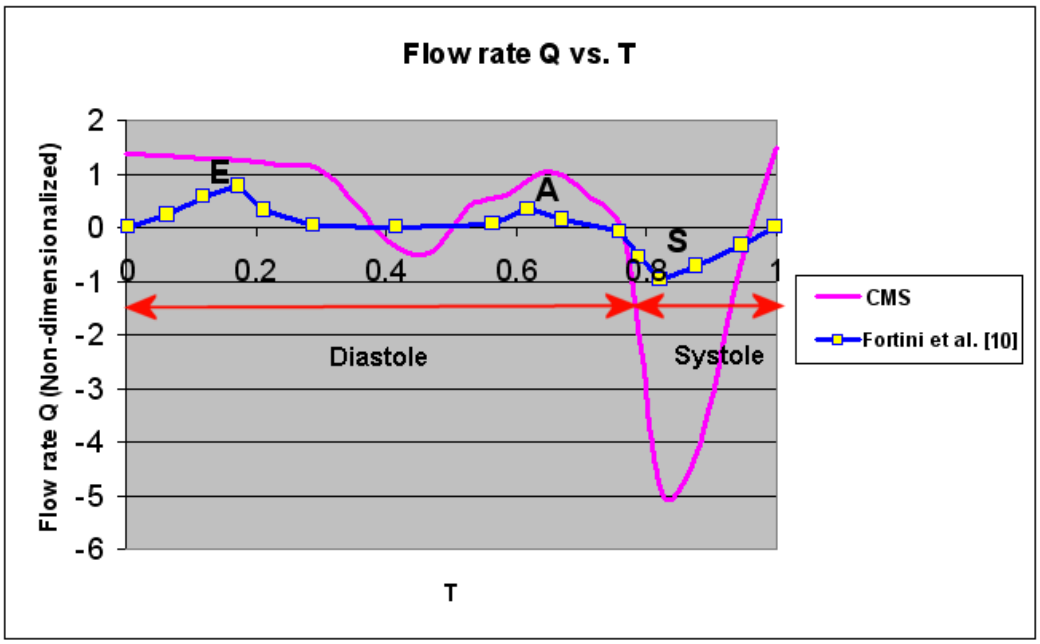

Fig. 5. Comparison between magnitudes of the inlet flow rate *Q* to the LV against time *t* plot, for CMS and Fortini et al. [7] . E, A and S refer to the E-wave, A-wave and S-wave respectively.

* The stroke volume refers to the difference in the volume of the LV between the end-diastolic and the end-systole phase and it can be obtained using the method outlined in the later vortex formation time section.

3.2 Analysis of vortex dynamic

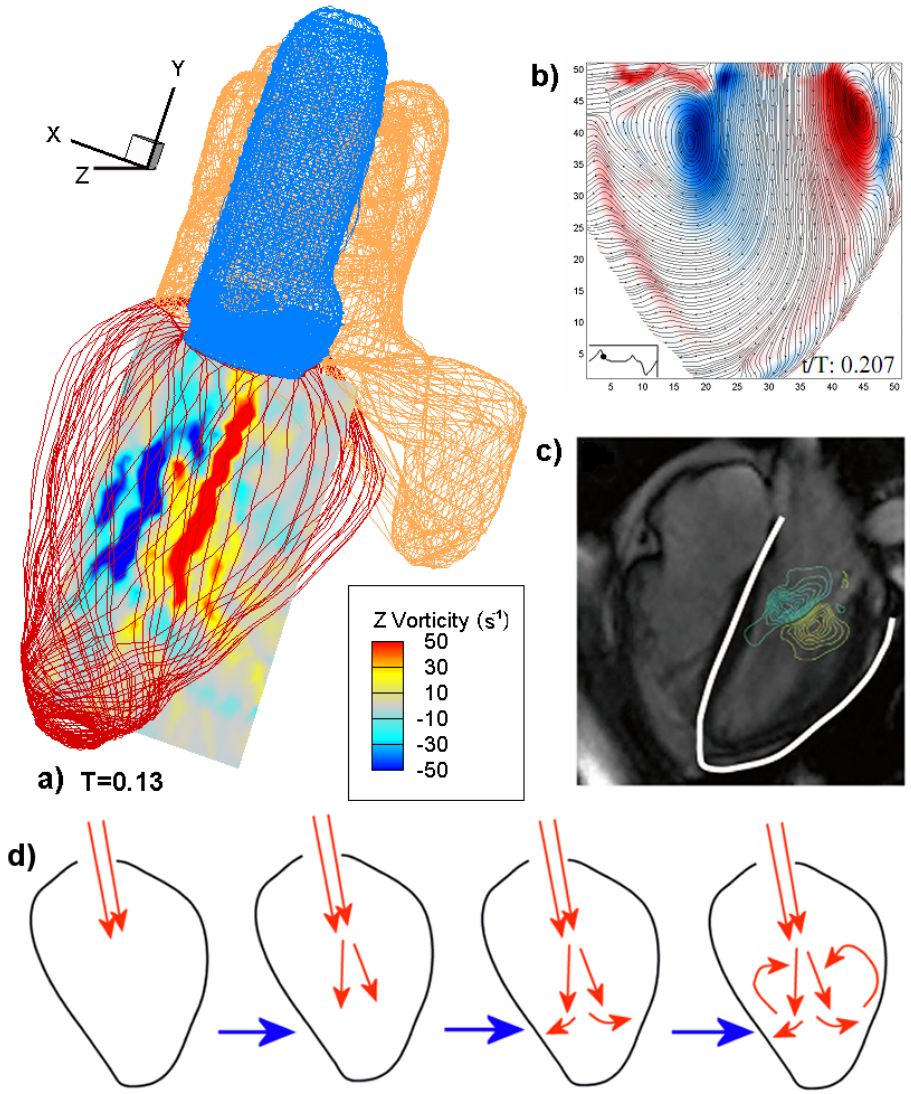

Fig. 6. a) Vorticity contour plots at z=0.56 (along same plane as PV location) at T=0.13. Experimental results of vorticity fields from b) Fortini et al. [7] and c) 4-D PC-MRI system. d) Simplified evolution of flow through a single axisymmetric opening valve

Fig. 6a shows the 2-D vorticity of CMS at T=0.13, which is around the early diastolic phase. The 2-D vorticity fields (Z vorticity) are obtained by extracting a slice of the heart along the z direction. Denoting the two edges of the heart as z=0 and z=1, the cross-section of the vorticity contour plot represents location z= 0.56 (Fig. 6a). This slice is chosen because it is on the same plane as the PV and can clearly show the vorticity variation. Blue and red represent negative and positive vorticities respectively. Note that the negative vortex is generated on the left while the positive one is on the right.

3.3 Kinetic energy

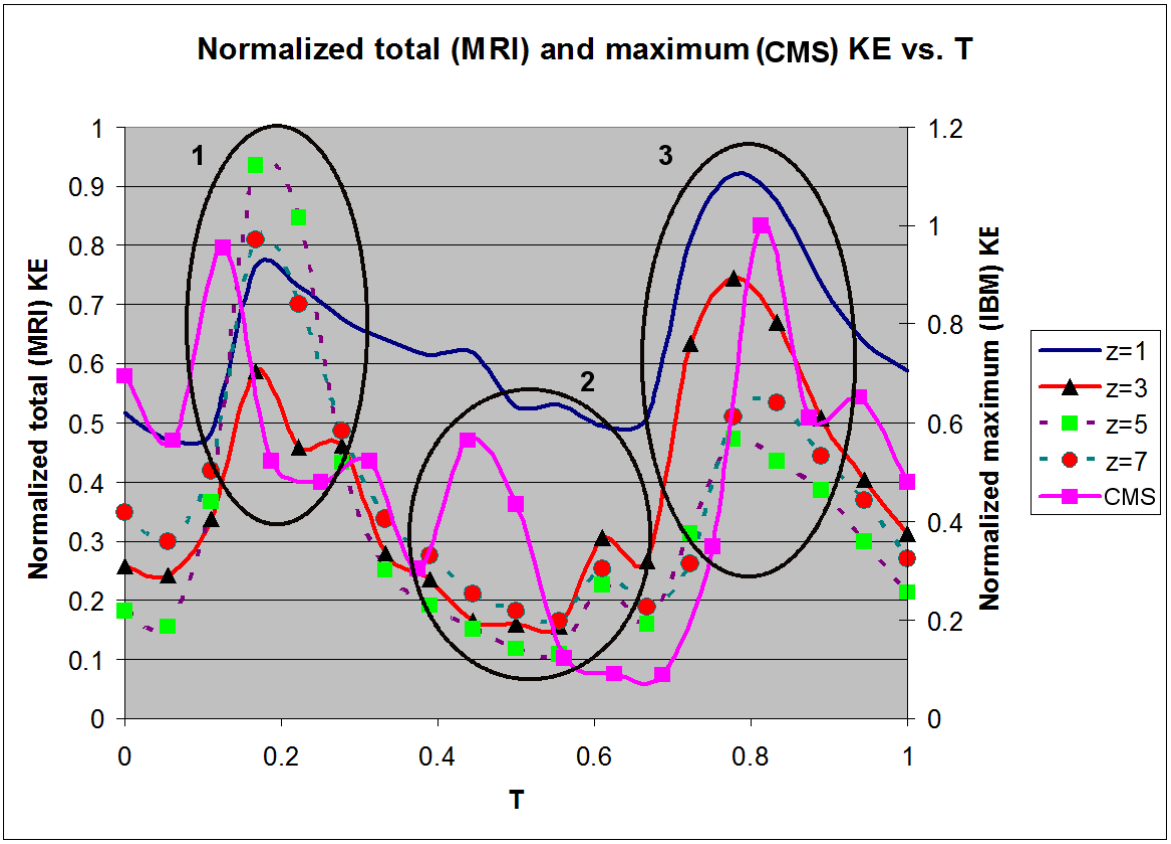

Fig. 7. Normalized total KE at different slices and maximum KE at slice z=0.56, obtained from the 4-D PC-MRI system and simulation respectively

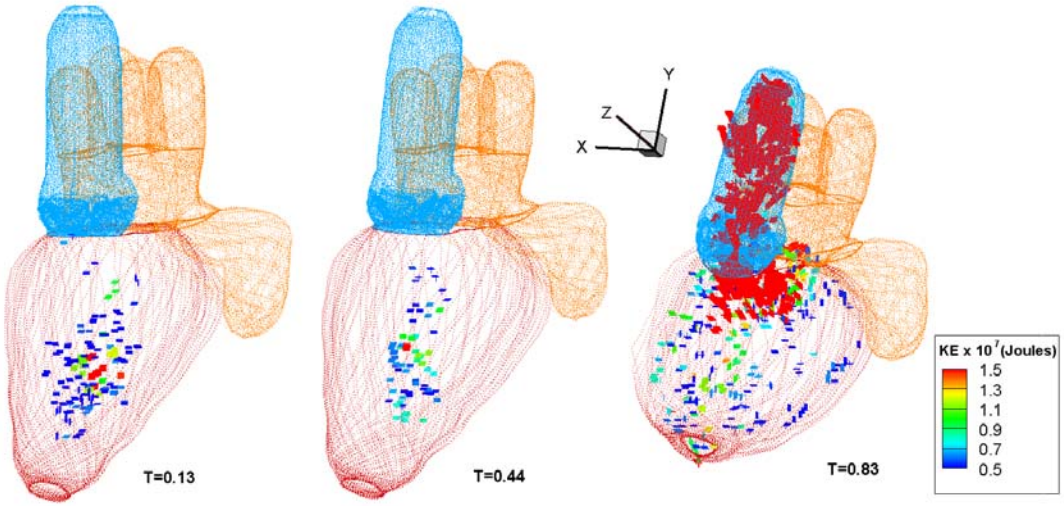

Fig. 8. KE of the markers in the LV for CMS at different times showing the three peaks. KE values below 3.0×10^{-7} joules are not shown. The color of the markers indicates the level of its KE.

The variation of the kinetic energy (KE) of the blood flow in the LV indicates the work done by the pumping heart. Fig. 7 shows the normalized maximum KE (at z=0.56) from the simulation and the total KE from the 4-D PC-MRI data for one cardiac cycle in the LV. The z=0.56 plane is selected because it can capture the variation of the KE

more clearly. Three peaks of the maximum KE can be observed at T=0.13, 0.44 and 0.83 (3 black circles 1-3). The actual locations where the maximum KE occurs can be observed in Fig. 8. It corresponds to a region of vorticity and energy.

4. Discussion

4.1 Hemodynamic comparison

We first discussed the flow rates through the PV and aorta in the simulation, with reference to Fig. 4. The large magnitudes shown by the red circle 3 (-50 cm^3/s) seem plausible. It seems that the magnitude should be similar to that of the earlier outflow (around T=0.45). This is because the mitral valve is closed at this time, as shown in the bottom left of Fig. 4 (small green circle). Hence, there is no additional blood travelling through the mitral valve to the LA and out to the PV. In an actual heart, the mitral valve opens to allow blood to flow into the LV during diastole, as shown by the green circle at the top right hand side of Fig. 4. Under normal condition, the mitral valve should prevent backflow during systolic phase. This shows that although the mitral valve is nearly closed, the 3-D heart model is not able to prevent backflow exactly during the systole phase (also known as mitral valve dysfunction). Further analysis of the similarity to the corresponding heart problems is required. It is interesting to note that in some diseased condition such as LV dilatation, mitral valve dysfunction or pulmonary arterial hypertension, large in/out flow variations are observed clinically, consistent with these idealized constant RPBC.

On the other hand, in Fig. 5, the comparison shows that the magnitude of the PV flow rate is generally twice as high as that of Fortini et al. [7]. The variation is also not so pronounced in the PV flow rate between T=0 and 0.3. It is only decreasing slowly and this is mainly due to the prolonged filling phase to ensure the momentum is balanced as mentioned earlier. For the aorta, comparison with flow data from Fortini et al.[7] show similar outflow during the systolic phase. The high outflow at the aorta occurs at a similar time (T=0.82). This indicates that the CMS can well simulate the different phases of the cardiac cycle. However, the aorta flow rate is much higher than that of Fortini et al.(-5.0 compared to -1.0). In Fortini et al.'s experiment, the inflow during diastole is similar to the outflow during systole. This is also true in the simulation, although its magnitude is much larger. This is most likely to conserve the prolonged filled mass flow rate numerically. Further investigation is still required to verify this speculation.

It is important to note that Fortini et al.'s graph in Fig. 5 is obtained by combining flow rate from the mitral value and aorta during the diastole and systole phase respectively. Hence, flow rates at the mitral valve and aorta during the systole and diastole phase are assumed to be zero respectively. But in the simulation, there is still outflow during the systole for the PV.

4.2 Analysis of vortex dynamic

The evolution of the vorticity in the LV throughout the entire cardiac cycle is discussed here. However, more emphasis is placed on the vorticity dynamics in the LV of the heart during diastole. As mentioned by Domenichini et al. [8], many researches [15, 16] have confirmed that the vortices generated in the LV play an important role in the heart functionality. Pierrakos and Vlachos [22] discussed the formation of vortex during the diastole period and showed that fluid transport is more efficient by vortex ring formation than a steady, straight jet of fluid.

The formation of the vortex and their respective locations can be explained using Fig. 6d). The blood flows into the LV through the mitral valve's opening. As the blood enters the LV, the larger space of the surrounding allows it to "spread" after traveling a short distance. Since the LV is still an enclosed space, the blood interacts with the wall and is constrained to "roll back" giving the vortices shown. Note that this is a simplified illustration of an axisymmetric valve but the valve in the modeled heart is non-axisymmetric. Numerous experiments have been conducted to show the pair of vortices. For example, Fortini et al. [7] tried to model the LV using conical sack made of silicone rubber and their results showed two vortices of opposite signs, similar to the simulation. The pair of vortices is also shown in the MRI image obtained from the 4-D PC-MRI system. Our simulation results tally well with the two experimental results (Fig. 6b) and c)). However, Fortini et al. [7] also argued that, as the diastolic phase

proceeds, the left negatively signed vortex (blue) would grow stronger than the right positively signed one. They suspected that the right (red) vortex interacts viscously with the wall of the LV, slows down and diminishes in size. This does not happen to the left (blue) vortex and hence it is able to grow bigger. Unfortunately, this is not observed in the current simulation. It is possible that the current code is not able to accurately simulate the viscous interaction of the vortex with the wall boundary. Finer mesh may be required.

4.3 Kinetic energy

From Fig. 7, we can observe that the first two timing (T=0.13 and 0.44) show that high volume of blood flows into the LV through the PV. This generates vortices which help to minimize the energy dissipation during flow transport [23]. The first peak corresponds to high inflow of the blood into the LV during the initial diastole (also known as E-wave) while the second lower peak (A-wave) corresponds to the period during atrial contraction. Since a higher flow rate is akin to higher kinetic energy, one can also compare with the flow rate against time plot in Fig. 5. These two peaks are also observed in the data by Fortini et al [7]. In this case, the peaks (E and A) occurred at around T=0.16 and 0.62 (interval of 0.46T). Hence, its time interval is also slightly longer. This may result from a number of possibilities. First of all, the data from the clinical data may not be universal due to the variations in patients, timing and others. From the simulation side, the imposed boundary conditions will influence the variation in KE as well. The third peak in Fig. 7 corresponds to the large outflow of oxygenated blood through the aorta valve during the systolic period. The same timing is also captured in Fig. 5, which is around T=0.83.

The normalized total KE of the heart using the 4-D PC-MRI system are also shown in Fig. 7. Due to the limitation of the system, it is not possible to obtain maximum KE only in the LV. Hence it is not possible to do a direct comparison for the two results in Fig. 7. Nevertheless, interesting information can be obtained by using slices of different planes. The z=5 (z=5 out of the 4 slices = 0.625) plane in this case is similar to the plane shown by the simulation result in Fig. 7 (z=0.56). There are also three peaks, with the second peak being less obvious (T=0.6). These correspond to the initial diastolic, atrial contraction and systolic phases. This shows that the simulation is able to show the peaks correctly. More investigations are required due to several uncertainties in either data or simulation (e.g. difference categories of volunteers such as male and female, age and the boundary conditions imposed).

5. Conclusions

Simulations have been carried out using the code by Mcqueen and Peskin [6] and the results are compared in terms of hemodynamic, vorticity visualization and kinetic energy analysis.

The variation of the flow rate in the PV and aorta compares well with the experimental data. The peaks during the E, A and S waves are captured by the simulation. However, the magnitudes do not tally well. Outflow is detected at the PV during the filling phase. This happens despite the mitral valve's closure. During systole, outflow occurs at the aorta due to oxygenated blood rushing out to different parts of the body.

Modeled vorticity fields show similar results as the experiments conducted by Fortini et al. [7]. Both simulation and experimental results show two oppositely signed vortices in the LV. However, the size difference of the left and right vortices is not captured by the simulation.

In terms of kinetic energy, the simulation results show similar number of peaks (three) as those found in the volunteer's result from the 4D PC-MRI system. The relative heights of the first two peaks (first higher than the second) are also correctly reflected when compared with the clinical data. Some minor differences between the KE and clinical data's flow rate are also seen. More investigations are required to determine if it is due to variance in the volunteer's data.

In general, the results show that using a simple RPBC gives a good comparison with clinical data in most analyisis. Further investigations are required to explain the reason behind some of the discrepancies. Future work includes changing the RPBC to investigate its effects on the flow rate, vorticity and KE. Comparison involving pressure and shear stress will be conducted too. Lastly, finer mesh will be used to do the simulation to obtain better accuracy. Further study will be presented.

References

[1] Bolzon, G., Zovatto, L., and Pedrizzetti, G., 2003, "Birth of Three-Dimensionality in a Pulsed Jet through a Circular Orifice," Journal of Fluid Mechanics, 493(pp. 209-218.

[2] Bellhouse, B. J., 1972, "Fluid Mechanics of a Model Mitral Valve and Left Ventricle," Cardiovascular Research, 6(2), pp. 199-210.

[3] Wieting, D. W., and Stripling, T. E., 1984, "Dynamics and Fluid Dynamics of the Mitral Valve," Recent Progress in Mitral Valve Disease, pp. 13-46.

[4] Reul, H., Talukder, N., and Muller, E. W., 1981, "Fluid-Mechanics of the Natural Mitral-Valve," Journal of Biomechanics, 14(5), pp. 361-&.

[5] Mcqueen, D. M., Peskin, C. S., and Yellin, E. L., 1982, "Fluid-Dynamics of the Mitral-Valve - Physiological-Aspects of a Mathematical-Model," American Journal of Physiology, 242(6), pp. 1095-1110.

[6] Mcqueen, D. M., and Peskin, C. S., 2000, "A Three-Dimensional Computer Model of the Human Heart for Studying Cardiac Fluid Dynamics," Computer Graphics-Us, 34(1), pp. 56-60.

[7] Fortini, S., Querzoli, G., Cenedese, A., and Marchetti, M., 2008,

[8] Domenichini, F., Pedrizzetti, G., and Baccani, B., 2005, "Three-Dimensional Filling Flow into a Model Left Ventricle," Journal of Fluid Mechanics, 539(pp. 179-198.

[9] Saber, N. R., Gosman, A. D., Wood, N. B., Kilner, P. J., Charrier, C. L., and Firmin, D. N., 2001, "Computational Flow Modeling of the Left Ventricle Based on in Vivo Mri Data: Initial Experience," Annals of Biomedical Engineering, 29(4), pp. 275-283.

[10] Kitajima, H. D., Sundareswaran, K. S., Teisseyre, T. Z., Astary, G. W., Parks, W. J., Skrinjar, O., Oshinski, J. N., and Yoganathan, A. P., 2008, "Comparison of Particle Image Velocimetry and Phase Contrast Mri in a Patient-Specific Extracardiac Total Cavopulmonary Connection," Journal of Biomechanical Engineering, 130(4), pp. 041004-14.

[11] Markl, M., Harloff, A., Bley, T. A., Zaitsev, M., Jung, B., Weigang, E., Langer, M., Hennig, J., and Frydrychowicz, A., 2007, "Time-Resolved 3d Mr Velocity Mapping at 3t: Improved Navigator-Gated Assessment of Vascular Anatomy and Blood Flow," Journal of Magnetic Resonance Imaging, 25(4), pp. 824-831.

[12] Who, 2002, *Integrated Management of Cardiovascular Risk*, World Health Organization,

[13] Abdallah, H., 2009, Pressures and the Heart: How Pressures Change in the Heart, 5th June, http://www.childrensheartinstitute.org/educate/bloodprs/prchange.htm

[14] Wikipedia, 2009, Superior Vena Cava 11th October, http://en.wikipedia.org/w/index.php?title=Superior_vena_cava&oldid=315757293

[15] Mandinov, L., Eberli, F. R., Seiler, C., and Hess, O. M., 2000, "Diastolic Heart Failure," Cardiovascular Research, 45(4), pp. 813-825.

[16] Vasan, R. S., and Levy, D., 2000, "Defining Diastolic Heart Failure - a Call for Standardized Diagnostic Criteria," Circulation, 101(17), pp. 2118-2121.

[17] Tseng, Y. H., and Ferziger, J. H., 2003, "A Ghost-Cell Immersed Boundary Method for Flow in Complex Geometry," Journal of Computational Physics, 192(2), pp. 593-623.

[18] Udaykumar, H. S., Mittal, R., Rampunggoon, P., and Khanna, A., 2001, "A Sharp Interface Cartesian Grid Method for Simulating Flows with Complex Moving Boundaries," Journal of Computational Physics, 174(1), pp. 345-380.

[19] Lai, M. C., and Peskin, C. S., 2000, "An Immersed Boundary Method with Formal Second-Order Accuracy and Reduced Numerical Viscosity," Journal of Computational Physics, 160(2), pp. 705-719.

[20] Baccani, B., Domenichini, F., Pedrizzetti, G., and Tonti, G., 2002, "Fluid Dynamics of the Left Ventricular Filling in Dilated Cardiomyopathy," Journal of Biomechanics, 35(5), pp. 665-671.

[21] Domenichini, F., Querzoli, G., Cenedese, A., and Pedrizzetti, G., 2007, "Combined Experimental and Numerical Analysis of the Flow Structure into the Left Ventricle," Journal of Biomechanics, 40(9), pp. 1988-1994.

[22] Pierrakos, O., and Vlachos, P. P., 2006, "The Effect of Vortex Formation on Left Ventricular Filling and Mitral Valve Efficiency," Journal of Biomechanical Engineering, 128(4), pp. 527-539.

[23] Kilner, P. J., Yang, G.-Z., Wilkes, A. J., Mohiaddin, R. H., Firmin, D. N., and Yacoub, M. H., 2000, "Asymmetric Redirection of Flow through the Heart," Nature, 404(6779), pp. 759-761.